

## ON A PERIODICALLY FORCED, WEAKLY DAMPED PENDULUM. PART 3: VERTICAL FORCING

PETER J. BRYANT<sup>1</sup> AND JOHN W. MILES<sup>2</sup>

(Received 12 May 1989; revised 18 October 1989)

### Abstract

We consider the phase-locked solutions of the differential equation governing planar motion of a weakly damped pendulum forced by a prescribed, vertical acceleration  $\varepsilon g \sin \omega t$  of its pivot, where  $\omega$  and  $t$  are dimensionless, and the unit of time is the reciprocal of the natural frequency. Resonance curves and stability boundaries are presented for downward and inverted oscillations of periods  $T, 2T, 4T, \dots$ , where  $T (\equiv 2\pi/\omega)$  is the forcing period. Stable, downward oscillations are found to occur in distinct regions of the  $(\omega, \varepsilon)$  plane, reminiscent of the regions of stability of the Mathieu equation (which describes the equivalent undamped, parametrically excited pendulum motion). The regions are dominated by oscillations of frequencies  $\frac{1}{2}\omega, \omega, \frac{3}{2}\omega, \dots$ , each region being bounded on one side by a vertical state at rest in stable equilibrium and on the other side by a symmetry-breaking, period-doubling sequence to chaotic motion. Stable, inverted oscillations are found to occur also in distinct regions of the  $(\omega, \varepsilon)$  plane, the principal oscillation in each region being symmetric with period  $2T$ .

### 1. Introduction

We consider a pendulum forced by a vertical acceleration  $\varepsilon g \sin \omega t$  of its pivot. The equation of motion is

$$\ddot{\theta} + 2\delta\dot{\theta} + \sin \theta = \varepsilon \sin \theta \sin \omega t, \quad (1.1)$$

where  $\theta$  is the angular displacement from the downward vertical,  $\delta$  is the damping ratio (actual/critical),  $\omega$  is the ratio of the forcing frequency to the natural frequency, and the unit of time is the inverse, natural frequency. We

<sup>1</sup>Department of Mathematics, University of Canterbury, Christchurch, New Zealand.

<sup>2</sup>Institute of Geophysics and Planetary Physics, University of California at San Diego, La Jolla, California 92093, U.S.A.

© Copyright Australian Mathematical Society 1990, Serial-fee code 0334-2700/90

assume  $\delta \ll 1$ ,  $\varepsilon = O(1)$  and  $\omega = O(1)$  in the analytic formulation based on a sinusoidal approximation for  $\theta$ , and set  $\delta = 1/8$  in the numerical calculations for the precise variation of  $\theta$ .

We have previously investigated the phase-locked solutions of a weakly damped pendulum forced by a periodic torque [2, 10], and by a horizontal periodic displacement of its pivot [3]. The same numerical method is used here for the vertically forced case. We develop solutions of (1.1) as truncated Fourier expansions containing a sufficient number of harmonics to render the numerical error arbitrarily small ( $< 10^{-4}$ ). In addition, a systematic numerical search was made of the asymptotic solutions in time of (1.1), using step-by-step integration with a local error tolerance of  $10^{-10}$ , to complement the Fourier series method. The chaotic solutions of (1.1) were not investigated further, since our primary focus is on the bifurcation structure. Previous numerical [6, 8] and experimental [7] studies of (1.1) have been concerned primarily with chaotic, rotational solutions of (1.1), whereas we are concerned primarily with periodic motions and their stability boundaries.

Symmetric and asymmetric swinging oscillations about both the downward vertical and the upward vertical and running oscillations with a mean angular velocity  $\langle \dot{\theta} \rangle$  ( $\langle \dot{\theta} \rangle / \omega$  is a rational number) are found, with periods that are multiples of the forcing period  $T$ . Resonance curves are defined, as before, as plots of  $\langle E \rangle^{1/2}$  vs  $\omega$ , where

$$E = \dot{\theta}^2/2 + 1 - \cos \theta \tag{1.2}$$

is a measure of the energy of oscillation. Stability is determined through the numerical integration of (1.1) with initial conditions close to those of the solution to be tested.

For undamped oscillations near the downward vertical ( $\delta = 0$ ,  $|\theta| \ll 1$ ), (1.1) may be rewritten as the Mathieu equation [1]

$$\theta'' + (p - 2q \cos 2v)\theta = 0 \tag{1.3a}$$

where

$$p = 4/\omega^2, \quad q = 2\varepsilon/\omega^2, \quad v = \omega t/2. \tag{1.3b,c,d}$$

The stability diagram in the  $qp$ -plane is sketched by Drazin and Reid [4], Figure 6.6 (after Abramowitz and Stegun [1], Figure 20.1). Parametric resonance, leading to unstable oscillations, occurs for small values of  $\varepsilon$  at forcing frequencies  $\omega$  near  $2/n$ ,  $n = 1, 2, \dots$ . A similar pattern occurs in the stability diagram for weakly damped oscillations (Figure 5), which also divides into regions associated with the forcing frequencies  $2/n$ ,  $n = 1, 2, \dots$ .

Resonance in the first region, at a forcing frequency twice the natural frequency, was observed originally by Faraday for surface waves on a fluid in a vertically oscillating container. The fluid has an infinite sequence of natural

frequencies, rather than the single natural frequency of the coplanar pendulum oscillation. For this reason, the more usual description of Faraday resonance is that the dominant oscillation of the fluid in the container occurs at half the frequency of the vertical oscillation of the container. Miles [9] developed an averaged Lagrangian formulation for the slowly varying amplitude of the primary mode of oscillation in weakly nonlinear Faraday resonance. The present fully nonlinear analysis of a forced pendulum with one degree of freedom is a first step towards a fully nonlinear analysis of Faraday resonance with many degrees of freedom, to complement the detailed experimental investigations by Gollub and Meyer [5], and others.

The oscillations in the first region are dominated by the harmonic with frequency  $\omega/2$  ( $\omega/2$  lies near 1 in this region), equivalent to period  $2T$ . Also, since (1.1) admits symmetric solutions satisfying

$$\theta(t + T) = -\theta(t), \quad (1.4)$$

a symmetric,  $2T$ -periodic oscillation is the first motion to occur on crossing the stability boundary from the vertical pendulum in stable equilibrium. As  $\omega$  is changed further, a symmetry-breaking stability boundary is crossed to stable, asymmetric,  $2T$ -periodic oscillations, followed by period-doubling stability boundaries. The period-doubling sequence terminates with a narrow band of nearly-periodic oscillations before chaotic oscillations or some independent periodic oscillations are reached.

The oscillations in the second region are dominated by the harmonic with frequency  $\omega$  ( $\omega$  lies near 1 in this region), equivalent to period  $T$ . Because (1.1) does not admit symmetric solutions satisfying

$$\theta\left(t + \frac{T}{2}\right) = -\theta(t), \quad (1.5)$$

an asymmetric,  $T$ -periodic oscillation is the first motion to occur on crossing the stability boundary from the vertical pendulum in stable equilibrium. As  $\omega$  is changed further, a period-doubling sequence of stable, asymmetric oscillations is followed until it terminates in the same manner as the first region.

The oscillations in the third region have the harmonic with frequency  $3\omega/2$  ( $3\omega/2$  lies near 1 in this region) of comparable magnitude to that of frequency  $\omega/2$ , with a period  $2T$ . This means that the first oscillations to occur are symmetric, with properties similar to those of the first region except that there are two dominant harmonics. This pattern continues on the stability diagram, with the odd regions having symmetric,  $2T$ -periodic oscillations on the threshold, and the even regions having asymmetric,  $T$ -periodic oscillations on the threshold.

The sinusoidal approximation reduces the oscillatory part of  $\theta$  to the dominant harmonic alone, and is applied successfully to the first region of the stability diagram. It provides a reasonable estimate for at least some of the resonance curves and stability boundaries.

The dominant regions of inverted oscillations describe motion that is symmetric with a period  $2T$ , having a mean  $\pi$  and amplitudes near, but less than,  $2\pi$ . Each region has a turning-point stability boundary on one side, and a symmetry-breaking stability boundary on the other side. The turning-point boundary marks a sudden transition to chaotic motion or some independent periodic motion. The symmetry-breaking boundary is followed by period-doubling boundaries.

A much narrower region of inverted oscillations has been found in which the motion is symmetric with a period  $2T$  and mean  $\pi$ , but with amplitudes near zero. This region is bounded on one side by a transition to a stable state of equilibrium in which the pendulum remains on the upward vertical from the pivot, and on the other side by a symmetry-breaking, period-doubling sequence. The region of inverted, stable equilibrium also is narrow, and is bounded on the other side by a transition to unstable,  $T$ -periodic, asymmetric, inverted oscillations with amplitudes near zero.

## 2. Downward oscillations of periods $T, 2T, \dots$

We represent  $mT$ -periodic oscillatory solutions of (1.1) by the Fourier series

$$\theta = \theta_0 + \sum_{k=1}^N [a_k \cos(k\omega t/m) + b_k \sin(k\omega t/m)], \tag{2.1}$$

where  $\theta_0$  is zero or near zero for downward oscillations, and  $a_k, b_k, k = 1, \dots, N$ , with  $\theta_0$  and  $N$  are determined numerically.

**2.1.  $2T$ -periodic oscillations.** The sinusoidal approximation for  $2T$ -periodic oscillations dominated by the lowest harmonic is

$$\theta = \theta_0 + \alpha \sin(\tau/2) \quad (\alpha > 0), \quad \tau = \omega t - \phi. \tag{2.2a,b}$$

When  $\theta$  is substituted into (1.1), and moments taken with respect to  $1, \cos(\tau/2), \sin(\tau/2)$ , we obtain

$$(J_0 - \epsilon J_2 \sin \phi) s_0 = 0, \tag{2.3a}$$

$$\delta \alpha^2 \omega = 4\epsilon J_2 c_0 \cos \phi, \tag{2.3b}$$

$$\alpha (\Omega c_0 - \omega^2/4) = -2\epsilon J_2' c_0 \sin \phi, \tag{2.3c}$$

where  $c_0 = \cos \theta_0$ ,  $s_0 = s \in \theta_0$ ,  $\Omega = 2J_1/\alpha$ , and the Bessel functions  $J_n$  are functions of  $\alpha$ . Equations (2.3a,b,c) admit five possibilities:

- (i)  $\theta_0 = \alpha = 0$ , downward vertical equilibrium;
- (ii)  $\theta_0 = 0$ ,  $\alpha > 0$ ,  $2T$ -periodic, symmetric, downward oscillations;
- (iii)  $\theta_0 \neq 0$ ,  $\alpha > 0$ ,  $2T$ -periodic, asymmetric, downward or inverted oscillations;
- (iv)  $\theta_0 = \pi$ ,  $\alpha = 0$ , upward vertical equilibrium;
- (v)  $\theta_0 = \pi$ ,  $\alpha > 0$ ,  $2T$ -periodic, symmetric, inverted oscillations.

The only question for (i) and (iv) concerns their stability. The inverted forms (iii) and (v) are described in Section 3, and attention here is directed first to (ii).

Setting  $\theta_0 = 0$  and eliminating  $\phi$  between (2.3b,c), we obtain

$$\left(\frac{\omega}{2}\right)^2 = \Omega - 2\delta^2 X^2 \pm X \left[ \left(\frac{4J_2}{\alpha^2}\right)^2 \varepsilon^2 - 4\delta^2 \Omega + 4\delta^4 X^2 \right]^{\frac{1}{2}} \tag{2.4}$$

where

$$\Omega = \frac{2J_1}{\alpha} = J_0 + J_2 = 1 - \frac{\alpha^2}{8} + \frac{\alpha^4}{192} + \dots, \tag{2.5a}$$

and

$$X = \frac{\alpha J_2'}{2J_2} = \frac{J_1 - J_3}{J_1 + J_3} = 1 - \frac{\alpha^2}{12} - \frac{\alpha^4}{576} + \dots \tag{2.5b}$$

Both  $\Omega$  and  $X$  are positive within the domain of the present approximation. The radical in (2.4) is real for  $0 \leq \alpha \leq \alpha_m$  where  $\alpha_m$  is the smallest root of

$$\delta \alpha^2 (\Omega - \delta^2 X^2)^{\frac{1}{2}} / (2J_2) = \varepsilon \quad (\alpha = \alpha_m). \tag{2.6}$$

The left side of (2.6) increases monotonically from  $\varepsilon_0$  at  $\alpha = 0$  to  $\varepsilon_*$  at  $\alpha = \alpha_* = 2.74 + 0(\delta^2)$ , where

$$\frac{\varepsilon_0}{4\delta} = (1 - \delta^2)^{\frac{1}{2}}, \quad \frac{\varepsilon_*}{4\delta} = 1.110[1 - 0.11\delta^2 + 0(\delta^4)], \tag{2.7a,b}$$

and then decreases to zero at  $\Omega = \delta^2 X^2$ . It follows (as is well known) that symmetric,  $2T$ -periodic oscillations are impossible if  $\varepsilon < \varepsilon_0$ .

The boundary between  $2T$ -periodic, symmetric oscillations and the downward vertical equilibrium state is given by the limit  $\alpha \rightarrow 0$  in (2.4),

$$(\omega/2)^2 = 1 - 2\delta^2 \pm (\varepsilon^2 - \varepsilon_0^2)^{\frac{1}{2}}/2. \tag{2.8}$$

The exact boundary obtained from a full Fourier series expansion is compared with (2.8) in Figure 1, where  $\delta = 1/8$ ,  $\varepsilon_0 = 0.496$ . The Fourier expansion for the  $2T$ -periodic symmetric oscillations is given by (2.1) with  $m = 2$ ,  $\theta_0 = 0$ , and  $a_{2k} = b_{2k} = 0$  for all  $k$ . The right, solid section of the exact

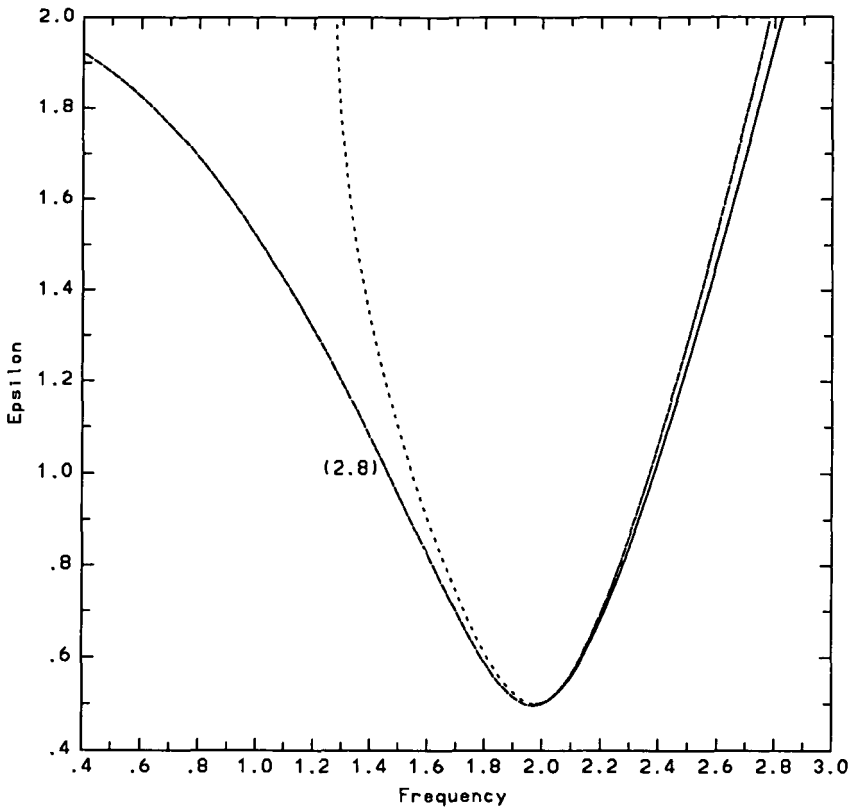


FIGURE 1. The stability boundary between the stable, downward vertical equilibrium state and the  $2T$ -periodic, symmetric oscillations. The oscillations are stable on the solid numerically calculated curves, unstable on the dotted numerically calculated curves, and the dashed curve is the approximate analytical result (2.8).

curve is a stability boundary between the stable, downward vertical equilibrium state on the right, and stable,  $2T$ -periodic, symmetric oscillations on the left, while the left, dotted section is a stability boundary between the stable, downward vertical equilibrium state on the left and unstable,  $2T$ -periodic, symmetric oscillations (coinciding with the unstable, downward equilibrium state) on the right. The approximate, dashed curve (2.8) provides a good fit to the stable section, but not to the upper part of the unstable section where higher harmonics become significant. The boundary equation (2.8) may be calculated also by a stability analysis of the downward vertical equilibrium state, using the Floquet method described previously ([10], Appendix A).

The resonance curve for symmetric  $2T$ -periodic oscillations with  $\varepsilon = 0.6$ ,  $\delta = 1/8$  is plotted in Figure. 2a. The exact resonance curve describes stable oscillations on the solid section to the turning point, and unstable oscilla-

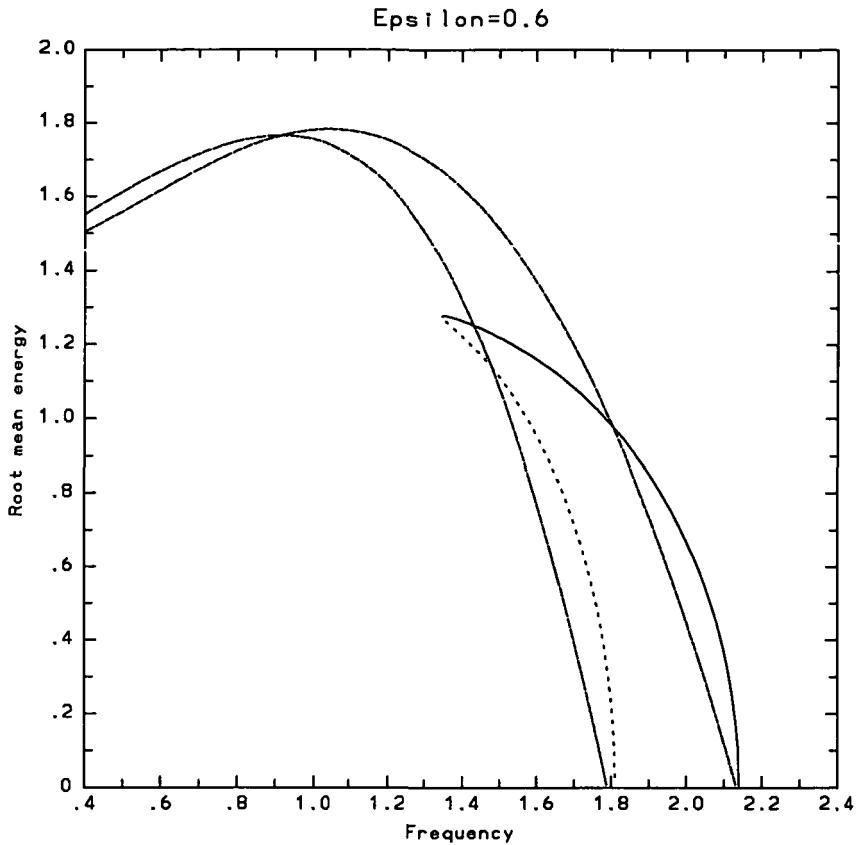


FIGURE 2a. The resonance curves for the  $2T$ -periodic, symmetric oscillations with  $\varepsilon = 0.6$ ,  $\delta = 1/8$ . The oscillations are stable on the solid numerically calculated curves, unstable on the dotted numerically calculated curves, and the dashed curves are the approximate analytical result (2.4).

tions on the following dotted section. The symmetric oscillations have an amplitude  $0.73\pi$  at the turning point. The approximate, dashed resonance curve is calculated from (1.2) with (2.4). The agreement is reasonable on the lower part of the curves, but fails on the upper part where higher harmonics become significant.

When  $\varepsilon$  is increased from the value 0.6 of Figure 2a, the oscillations become unstable on the right part of the resonance curve before the turning point is reached. Change of stability occurs at a symmetry-breaking point, the stable state being asymmetric,  $2T$ -periodic oscillations in a neighbourhood beyond the point. An example of such a resonance curve at  $\varepsilon = 1.0$ ,  $\delta = 1/8$

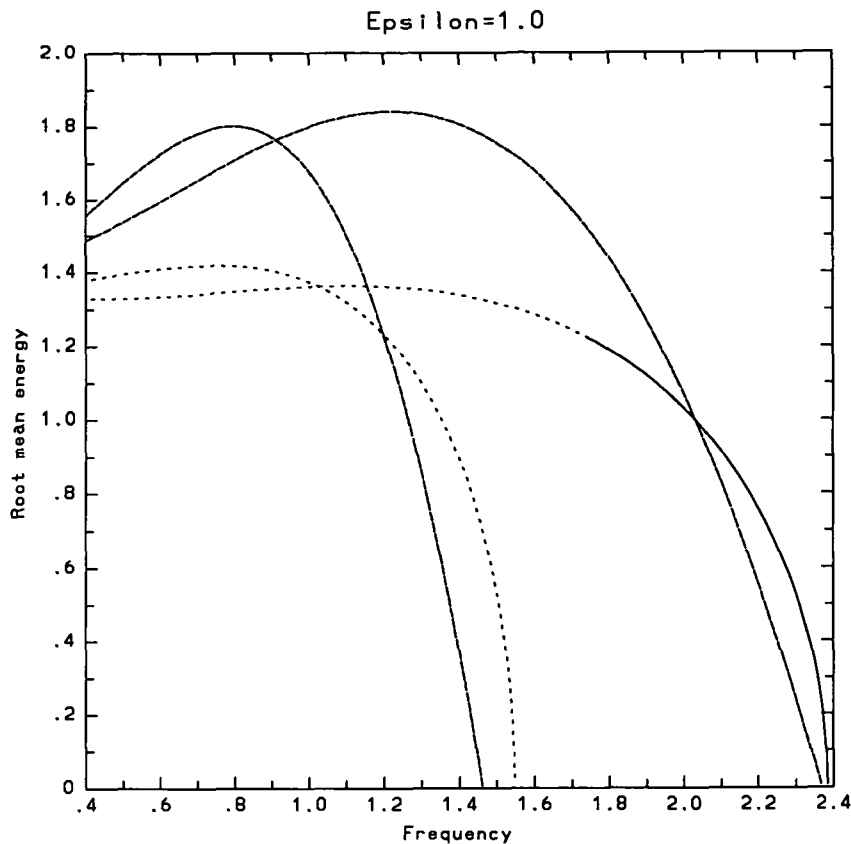


FIGURE 2b. The resonance curves for the  $2T$ -periodic, symmetric oscillations with  $\varepsilon = 1.0$ ,  $\delta = 1/8$ .

is shown in Figure 2b. The right part of the exact resonance curve describes stable oscillations on the solid section to the symmetry-breaking point at  $\omega = 1.735$ ,  $\langle E \rangle^{\frac{1}{2}} = 1.227$ , where the symmetric oscillations have an amplitude  $0.64\pi$ . The approximate, dashed resonance curve from (1.2) and (2.4) agrees only with the lower part of the exact curves.

Multiple resonance curves appear as  $\varepsilon$  is increased further from the value 1.0 in Figure 2b. The resonance curves at  $\varepsilon = 2.0$ ,  $\delta = 1/8$  are sketched in Figure 2c. Stable sections are shown on the first and third curves from the right, in each case bounded above by a symmetry-breaking point. The approximate resonance curve (not drawn) agrees with the lower part of the first curve only.

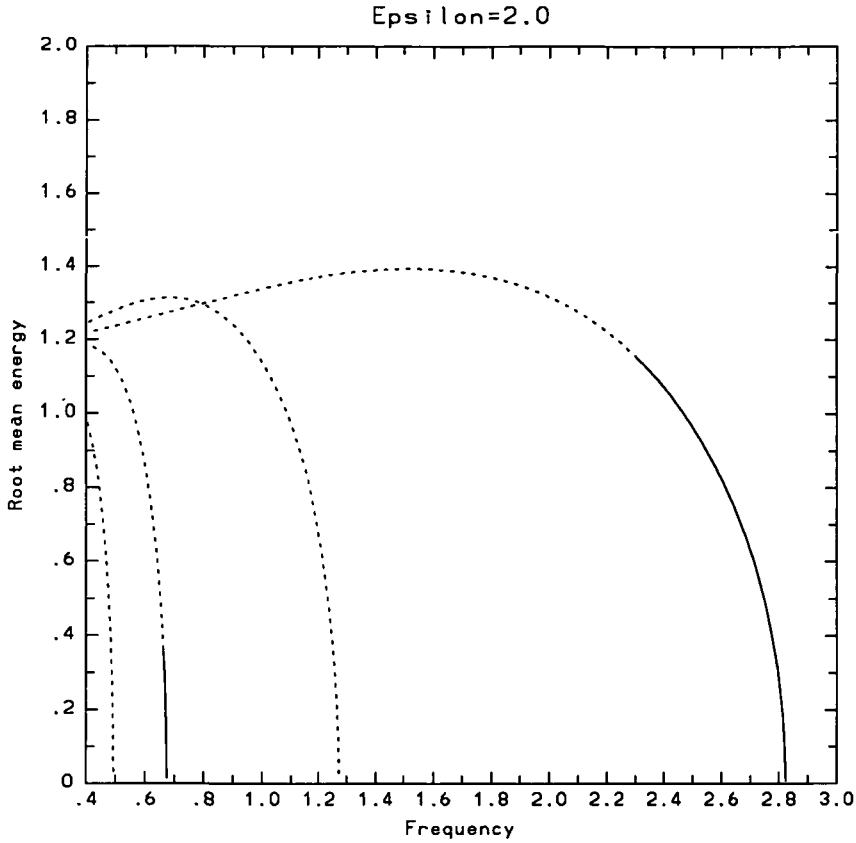


FIGURE 2c. The resonance curves for the  $2T$ -periodic, symmetric oscillations with  $\epsilon = 2.0$ ,  $\delta = 1.8$ .

We obtain asymmetric,  $2T$ -periodic oscillations by eliminating  $\phi$  among (2.3a,b,c) on the hypothesis that  $s_0 \neq 0$  when

$$\left(\frac{J_0}{J_2}\right)^2 + \left(\frac{\delta\alpha^2\omega}{4J_2c_0}\right)^2 = \epsilon^2, \tag{2.9a}$$

$$c_0 = \frac{\alpha^2\omega^2}{4(\alpha^2\Omega + 4XJ_0)}. \tag{2.9b}$$

The symmetry-breaking bifurcation ( $c_0 = 1$ ,  $J_0 + \epsilon J_2 \sin \phi = 0$ ) is determined by

$$\epsilon^2 = \left(\frac{J_0}{J_2}\right)^2 + \frac{\delta^2\alpha^2(\alpha^2\Omega + 4XJ_0)}{4J_2^2} \quad (\alpha = \alpha_s), \tag{2.10a}$$

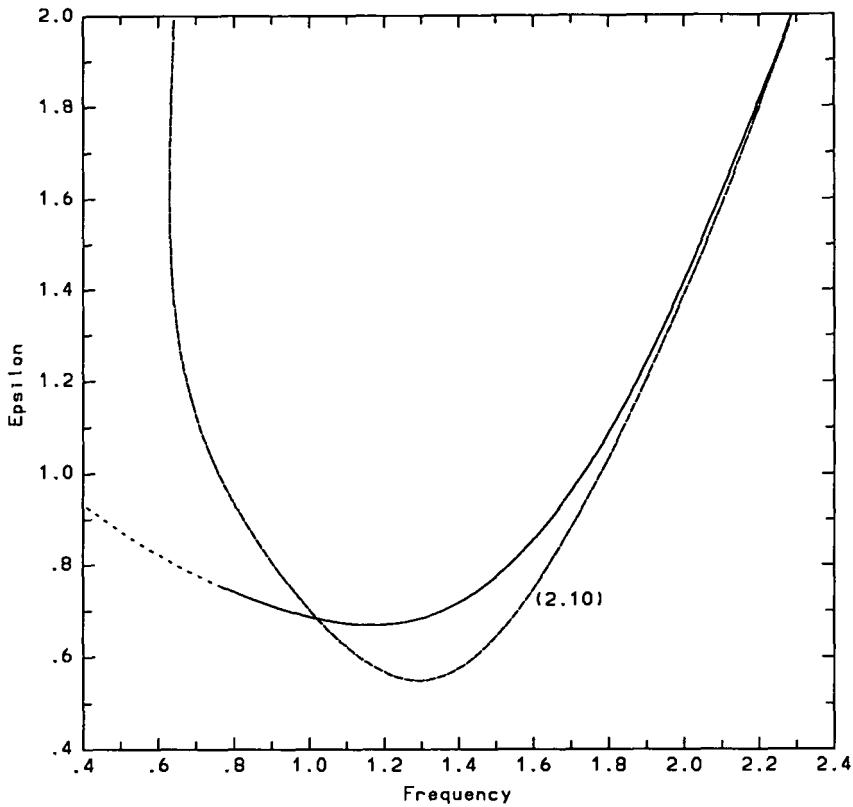


FIGURE 3. The symmetry-breaking curves for  $2T$ -periodic oscillations. The oscillations are stable on the solid numerically calculated curves, unstable on the dotted numerically calculated curves, and the dashed curve is the approximate analytical result (2.10).

$$\omega = \frac{2(\alpha^2 \Omega + 4XJ_0)^{\frac{1}{2}}}{\alpha} \quad (\alpha = \alpha_s). \tag{2.10b}$$

Equation (2.10) is compared in Figure 3 with the exact symmetry-breaking curve for the right part of the resonance curves. The fit is excellent at the larger values of  $\omega$ , where  $\theta$  is dominated by the first harmonic, but fails at smaller  $\omega$  where higher harmonics are significant.

**2.2.  $T$ -periodic oscillations.** The full Fourier expansion for  $T$ -periodic, asymmetric oscillations is given by (2.1) with  $m = 1$ ,  $\theta_0$  near zero, and both even and odd harmonics present. If the Fourier expansion is substituted into (1.1) for solutions satisfying  $|\theta| \ll 1$  when  $\varepsilon = 0(1)$ , it may be shown that the mean  $\theta_0$  and the second harmonic are of comparable magnitude, although dominated by the first harmonic. This means that there is

no simple sinusoidal approximation like (2.2), with  $\theta_0 \neq 0$ , from which the principal results for  $T$ -periodic asymmetric oscillations may be estimated with reasonable accuracy using the moment method. Equation (1.1) does not admit symmetric,  $T$ -periodic solutions satisfying (1.5), leaving 4 relevant possibilities:

- (i)  $\theta = 0$ , all  $t$ , downward vertical equilibrium;
- (ii)  $T$ -periodic, asymmetric, downward oscillations ( $\theta_0$  near zero);
- (iii)  $T$ -periodic, asymmetric, inverted oscillations ( $\theta_0$  near  $\pi$ );
- (iv)  $\theta = \pi$ , all  $t$ , upward vertical equilibrium.

The first two possibilities are described here and the other two in Section 3. Calculations with full Fourier expansions show that the minimum value of  $\varepsilon$  for  $T$ -periodic oscillations when  $\delta = 1/8$  is 1.0002, and that  $\omega = 0.915$  at this point.

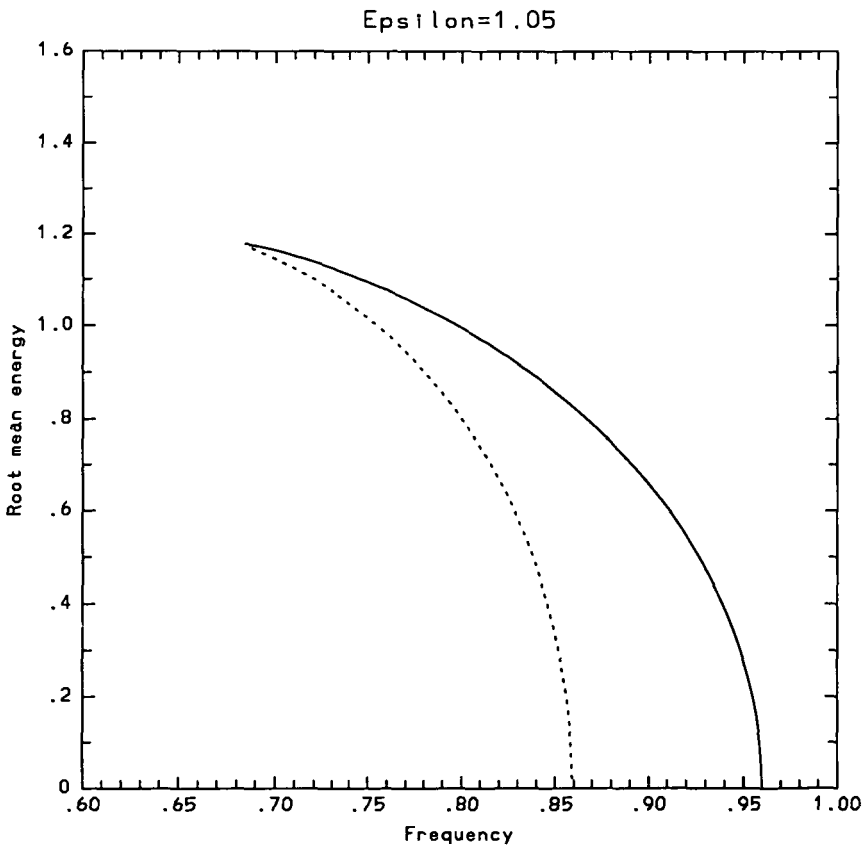


FIGURE 4a. The resonance curve for the  $T$ -periodic, asymmetric oscillations with  $\varepsilon = 1.05$ ,  $\delta = 1.8$ .

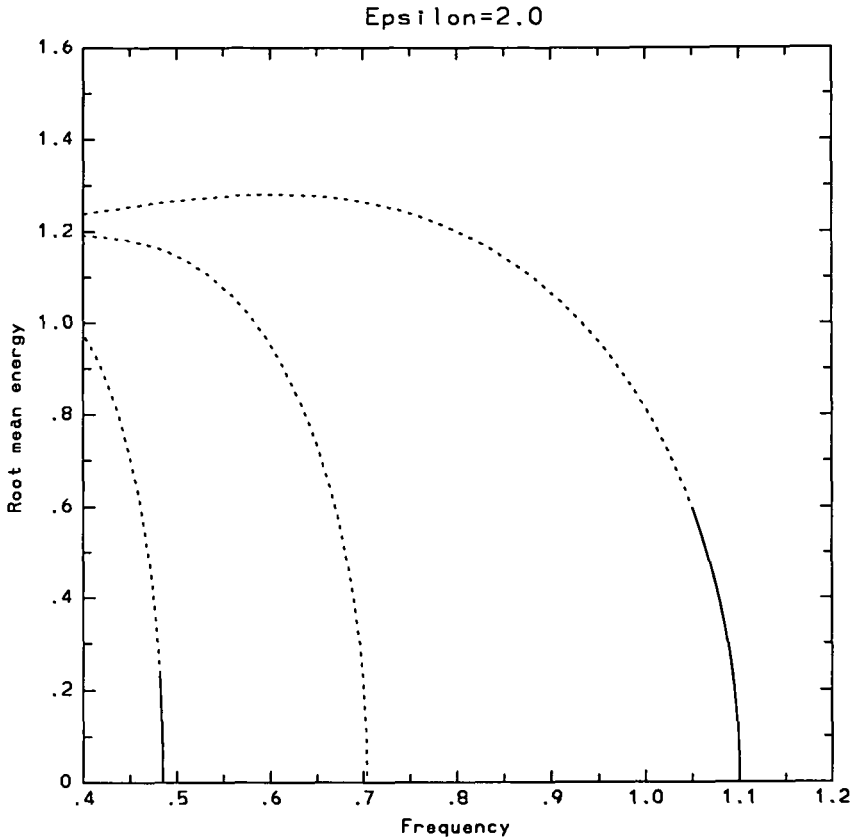


FIGURE 4b. The resonance curves for the  $T$ -periodic, asymmetric oscillations with  $\varepsilon = 2.0$ ,  $\delta = 1.8$ .

The resonance curve for  $T$ -periodic, asymmetric oscillations when  $\varepsilon = 1.05$ ,  $\delta = 1/8$  is sketched in Figure 4a, which has a similar form to Figure 2a. The oscillations are stable on the right solid section, to the turning point, and are unstable on the left, dotted section. Like the  $2T$ -periodic oscillations, there are an increasing number of resonance curves as  $\varepsilon$  is increased beyond the value in Figure 4a. The resonance curves for  $\varepsilon = 2.0$ ,  $\delta = 1/8$  are drawn in Figure 4b. As in Figure 2c, each of the stable, solid sections of the resonance curves is bounded by a point where the  $T$ -periodic oscillations become unstable. However, unlike Figure 2c, these points are period-doubling points, dividing the stable,  $T$ -periodic, asymmetric oscillations from stable,  $2T$ -periodic, asymmetric oscillations.

**2.3. Stability.** The regions of stability for the  $2T$ -periodic and  $T$ -periodic oscillations described above, and their descendants, are summarised in Figure 5.

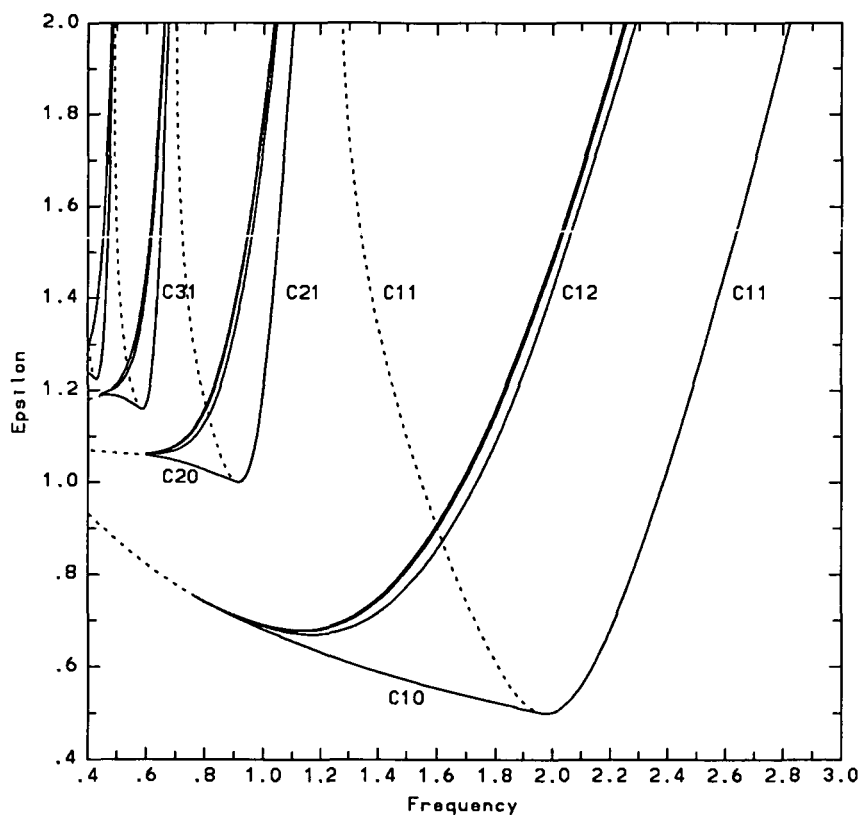


FIGURE 5. The stability diagram for  $T, 2T, 4T, \dots$ -periodic oscillations, with  $\delta = 1/8$ . The notation is described in Section 2.3.

Stability is determined for any particular solution by calculating numerically the asymptotic solution of (1.1) from initial conditions in the neighborhood of the solution. Attention is drawn to the similarity in structure from right to left across the figure, reminiscent of the similarity in structure of the stability diagram for the Mathieu equation (1.3), illustrated in [4], Figure 6.6. This is to be expected, since the Mathieu equation describes the undamped form of the present forced pendulum motion for small oscillations.

The curve  $C_{11}$  in the right region is the same as that in Figure 1, dividing the symmetric  $2T$ -periodic oscillations on the inside from the stable, downward vertical equilibrium state on the outside of the curve. The part of the symmetric,  $2T$ -periodic oscillations on the inside of the left, dotted section of  $C_{11}$  is unstable, shown as the first dotted curve rising from  $\langle E \rangle^{\frac{1}{2}} = 0$  in

Figures 2a,b,c. When the stable part that begins on the right solid section of  $C_{11}$  is followed to the left in the figure, it is terminated either at the turning-point curve  $C_{10}$ , as for the solid curve rising from  $\langle E \rangle^{\frac{1}{2}} = 0$  in Figure 2a, or at the symmetry-breaking curve  $C_{12}$ , as for the first solid curve rising from  $\langle E \rangle^{\frac{1}{2}} = 0$  in Figures 2b,c. In the lower triangular section between the  $C_{12}$ ,  $C_{10}$ , and dotted  $C_{11}$  curves, symmetric,  $2T$ -periodic oscillations and the downward vertical equilibrium state are both stable.

The symmetry-breaking curve  $C_{12}$  is the same as that in Figure 3. It is followed by a narrow band of stable, asymmetric,  $2T$ -periodic oscillations, which become unstable in turn on the period-doubling curve  $C_{14}$ . This curve is a stability boundary for asymmetric,  $4T$ -periodic oscillations, bounded on the other side by the next period-doubling curve  $C_{18}$ . The period-doubling sequence degenerates into a band of nearly-periodic motion as  $\omega$  is decreased further, merging into either an independent periodic motion or chaotic motion. All the oscillations within the first region of Figure 5 are dominated by the harmonic of frequency  $\omega/2$ , where  $\omega$  lies near 2.

The curve  $C_{21}$  in the next region of Figure 5 divides the asymmetric,  $T$ -periodic oscillations on the inside from the stable, downward vertical equilibrium state on the outside of the curve. The stable and unstable sections of the curve  $C_{21}$  have the same function as in the first region, except that the oscillations inside are asymmetric and  $T$ -periodic, rather than symmetric and  $2T$ -periodic, and are described by the first two curves rising from  $\langle E \rangle^{\frac{1}{2}} = 0$  on Figures 4a,b.  $C_{22}$  is a period-doubling curve, followed by the period-doubling sequence  $C_{24}$ ,  $C_{28}$ , ... . All the oscillations within this second region of Figure 5 are dominated by the frequency  $\omega$ , where  $\omega$  lies near 1.

The third region is like the first region in Figure 5, with the curve  $C_{31}$  dividing symmetric,  $2T$ -periodic oscillations on the inside from the downward vertical equilibrium state on the outside of the curve, and the remaining curves having the same roles as in the first region. The difference from the first region is that the harmonic with frequency  $3\omega/2$  is of comparable magnitude to that of frequency  $\omega/2$ , where  $3\omega/2$  lies near 1. The fourth region is like the second region in Figure 5, with  $T$ -periodic, asymmetric oscillations inside the curve  $C_{41}$ , and the harmonic with frequency  $2\omega$  of comparable magnitude to that of frequency  $\omega$ , where  $2\omega$  lies near 1.

The regions in Figure 5 continue to alternate between  $2T$ -periodic and  $T$ -periodic oscillations as the threshold oscillating state, for decreasing  $\omega$  across the figure, with the harmonic of frequency  $n\omega/2$  having an important role in the  $n$ th region, where  $n\omega/2$  lies near 1. The closer proximity of successive regions below  $\omega = 0.4$  in Figure 5 makes the calculation of precise stability boundaries more difficult there.

### 3. Inverted oscillations of periods $T, 2T, \dots$

We represent  $mT$ -periodic, inverted, oscillatory solutions of (1.1) by the Fourier series (2.1) with  $\theta_0$  equal to  $\pi$  or near  $\pi$ .

**3.1.  $2T$ -periodic oscillations.** The stability diagram for inverted,  $2T$ -periodic oscillations and their descendants is sketched in Figure 6. The boundary curve  $C_0$  on each band is a turning-point curve, on which the amplitude of oscillation is much larger than zero. In the first band, the  $2T$ -periodic, stable, symmetric oscillation on the turning-point boundary  $C_0$  at  $\varepsilon = 1.5$ ,  $\omega = 0.855$ , has an amplitude  $1.45\pi$ , oscillating between  $-0.45\pi$  and  $2.45\pi$ . When  $\omega$  is decreased, the symmetry-breaking curve  $C_2$  is reached, beyond which the stable, asymptotic state is  $2T$ -periodic, asymmetric oscillations. As  $\omega$  is decreased further, the period-doubling sequence  $C_4, C_8, \dots$  is followed before nearly-periodic, inverted oscillations are reached, then an independent periodic motion or chaotic motion. At  $\varepsilon = 1.5$ , for example,  $4T$ -periodic, inverted oscillations extend from  $\omega = 0.782$  to  $0.779$ , an  $8T$ -periodic, inverted oscillation occurs at  $\omega = 0.778$ , then nearly-periodic, inverted oscillations extend from  $\omega = 0.777$  to  $0.770$ , followed by chaotic motion.

The same form of symmetry-breaking, period-doubling sequence is followed in the second band of inverted,  $2T$ -periodic oscillations in Figure 6. The symmetric oscillation on the turning point boundary  $C_0$  at  $\varepsilon = 1.5$ ,  $\omega = 0.418$ , has an amplitude  $1.36\pi$ , oscillating between  $-0.36\pi$  and  $2.36\pi$ . It has a second minimum and maximum within each period, where  $\theta$  is equal to  $-0.23\pi$  and  $2.23\pi$  respectively. There is a third band of inverted,  $2T$ -periodic oscillations to the left of Figure 6. The symmetric oscillation on the turning point boundary  $C_0$  at  $\varepsilon = 1.5$ ,  $\omega = 0.238$ , has three maxima and minima in each period, the three maxima being  $2.31\pi$ ,  $2.16\pi$ ,  $2.12\pi$ .

**3.2. Upward vertical equilibrium state.** Equation (1.1) admits vertical solutions for which  $\theta = \pi$  for all  $t$ . It also admits  $T$ -periodic, asymmetric, inverted, oscillatory solutions for which  $m = 1$  and  $\theta_0$  lies near  $\pi$  in (2.1). A systematic search of the asymptotic solutions to (1.1) did not find any stable,  $T$ -periodic, inverted, oscillatory solutions, but it did find a very narrow band in which the upward vertical equilibrium state is stable. Curiously, this stable band is bounded on one side by unstable,  $T$ -periodic, inverted oscillations of small amplitude. A narrow band of stable, symmetric,  $2T$ -periodic, inverted oscillations of small amplitude is found on the other side of the equilibrium region, followed by a very narrow symmetry-breaking and period-doubling sequence of stable, inverted oscillations of small amplitude. The location of this region is shown in Figure 7.

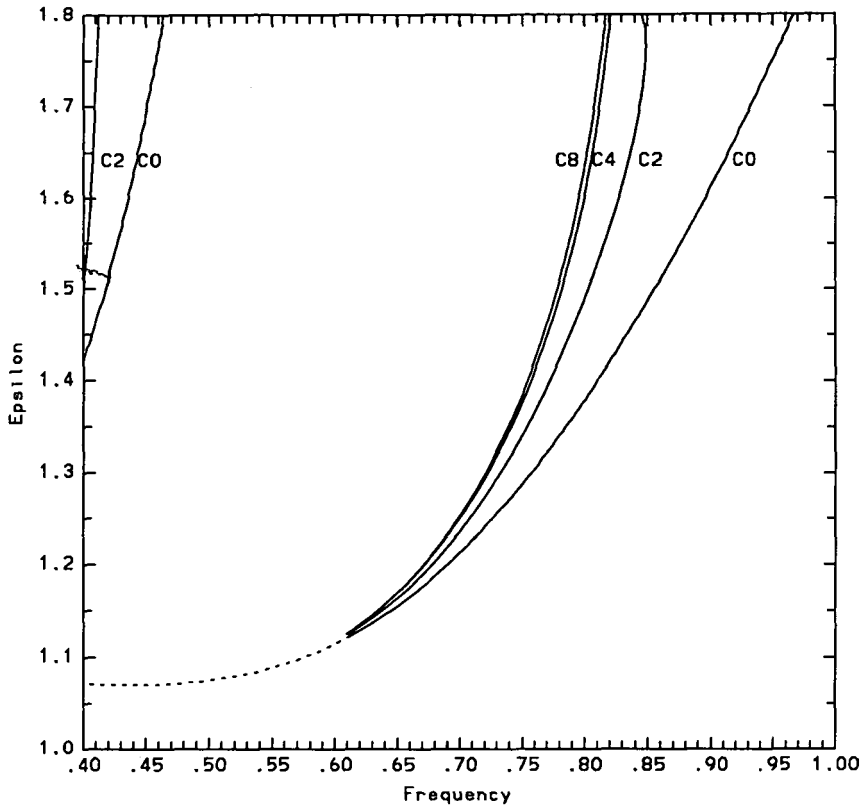


FIGURE 6. The stability diagram for  $2T, 4T, \dots$ -periodic inverted oscillations, with  $\delta = 1/8$ . The notation is described in Section 3.1.

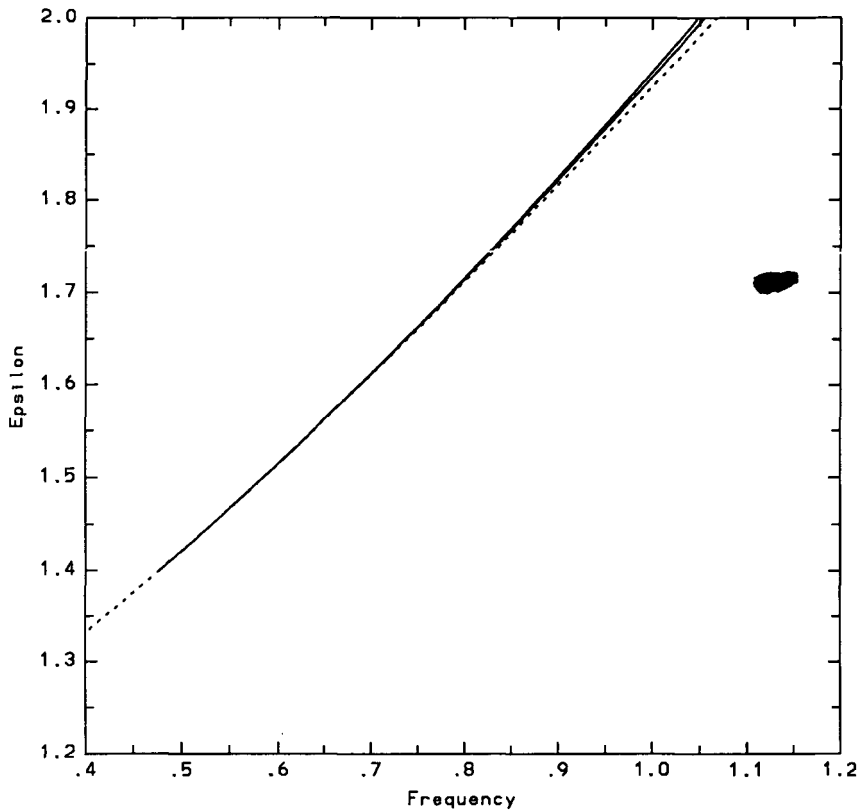


FIGURE 7. The stability diagram for the stable, inverted equilibrium state and for the  $2T$ ,  $4T$ , ...-periodic inverted oscillations with amplitudes near zero. The equilibrium state occurs between the dotted curve and the first solid curve.

#### 4. Further stable oscillations

Like the other two cases of forced, weakly damped pendulum oscillation [2, 3], there is a wide range of stable, oscillatory motions that occur here. A broad region of stable, running,  $T$ -periodic oscillations with mean angular velocity  $\omega$  exists, for example, bounded on one side by a turning-point stability curve, and on the other side by a period-doubling sequence. Typical of the more unusual running oscillations is a  $3T$ -periodic oscillation with a mean angular velocity  $\omega/3$ .

One noticeable feature in comparing this case with the previous two cases of forced pendulum motion is the scarcity of stable oscillations with periods that are odd multiples of  $T$ , the main exceptions being the  $T$ -periodic asymmetric oscillations described in Section 2.2 and the  $T$ -periodic running

oscillations mentioned above. In these previous cases, there were broad regions of  $3T$ -periodic, swinging oscillations, both downward and inverted. A systematic search of the stable, oscillatory motions in the present case did not find a single example of a  $3T$ -periodic, swinging oscillation, although (1.1) does admit  $3T$ -periodic, asymmetric, swinging oscillatory solutions.

## 5. Summary

Small amplitude periodic oscillations of a damped pendulum are symmetric about the vertical when the pendulum is torque-driven (Part 1) or forced horizontally (Part 2). If it is driven vertically (Part 3) with a force of small amplitude, any initial motion is damped to leave the pendulum in vertical equilibrium. This stable vertical state exists with, or is replaced by, either symmetric or asymmetric oscillations once the vertical driving amplitude passes a threshold (Part 3, Figure 5). Symmetric oscillations lose stability to asymmetric oscillations when the forcing amplitude is increased, these in turn lose stability to asymmetric oscillations of twice the period at a greater forcing amplitude, and so on in period-doubling sequences. No examples were found of period-doubling occurring before symmetry-breaking, and when stable symmetric oscillations of twice the period do exist, they appear to be independent of the single period symmetric oscillations. Period-doubling sequences were found to terminate in a small interval in which the oscillations are nearly-periodic, with  $(\theta, \dot{\theta})$ -orbits close to those in the sequence. This property persisted for numerical solutions of the governing differential equation to large times even when the local error tolerance was reduced to  $10^{-11}$ , but it may need higher precision than this to be understood fully.

The remarkable feature of the three cases of forced, damped, coplanar pendulum motion examined here is the kaleidoscope of different stable, periodic oscillations that can occur. Stable oscillations can be found with periods at all low integer multiples of the forcing period, with symmetric or asymmetric motion about the vertical, with downward or inverted means, and with zero or nonzero mean angular velocities (an integer number of rotations over sufficient forcing periods). Each periodic oscillation is determined by the values of amplitude and frequency at which the pendulum is forced, and by the initial state of the pendulum. All these different periodic oscillations occur for the coplanar pendulum with only one degree of freedom, anticipating an even greater variety of periodic oscillations for dynamical systems with many degrees of freedom.

### Acknowledgement

This work was supported in part by the Physical Oceanography, Applied Mathematics and Fluid Dynamics/Hydraulics programs of the National Science Foundation, NSF Grant OCE-81-17539, by the Office of Naval Research, Contract N00014-84-K-0137,4322318(430), and by the DARPA Univ. Res. Init. under Appl. and Comp. Math. Program Contract N00014-86-K-0758 administered by the Office of Naval Research, and by a grant of computing time from the San Diego Supercomputer Center (sponsored by the National Science Foundation) [which was used for an accurate, systematic search of the asymptotic solutions in time of (1.1)].

### References

- [1] M. Abramowitz and I. A. Stegun (eds.), *Handbook of Mathematical Functions* (Dover, New York, 1970), 722ff.
- [2] Peter J. Bryant and John W. Miles, "On a periodically forced, weakly damped pendulum. Part 1: Applied torque", *J. Austral. Math. Soc. Ser. B.* **32** (1990) 1–22.
- [3] Peter J. Bryant and John W. Miles, "On a periodically forced, weakly damped pendulum. Part 2: Horizontal forcing", *J. Austral. Math. Soc. Ser. B.* **32** (1990) 23–41.
- [4] P. G. Drazin and W. H. Reid, *Hydrodynamic Stability* (Cambridge University Press, 1981), 357.
- [5] J. P. Gollub and Christopher W. Meyer, "Symmetry-breaking instabilities on a fluid surface", *Physica D* **6** (1983) 337–346.
- [6] R. W. Leven and B. P. Koch, "Chaotic behaviour of a parametrically excited damped pendulum", *Phys. Lett. A* **86** (1981) 71–74.
- [7] R. W. Leven, B. Pompe, C. Wilke and B. P. Koch, "Experiments on periodic and chaotic motions of a parametrically forced pendulum", *Physica D* **16** (1985) 371–384.
- [8] J. B. McLaughlin, "Period-doubling bifurcations and chaotic motion of a parametrically forced pendulum", *J. Stat. Phys.* **24** (1981) 375.
- [9] John W. Miles, "Nonlinear Faraday resonance", *J. Fluid Mech.* **146** (1984) 285–302.
- [10] John W. Miles, "Resonance and symmetry breaking for the pendulum", *Physica D* **31** (1988) 252–268.